Arc controls alcohol cue relapse by a central amygdala mechanism

Kasia Radwanska (k.radwanska@nencki.edu.pl)
Nencki Institute

Roberto Pagano
Nencki Institute

Ahmad Salamian
Laboratory of Molecular Basis of Behavior, Nencki Institute, Warsaw, Poland https://orcid.org/0000-0003-2841-9228

Janusz Zielinski

Anna Beroun
Nencki Institute

Maria Nalberczak-Skóra
Nencki Institute

Edyta Skonieczna
Nencki Institute

Anna Cały
Nencki Institute of Experimental Biology (PAS) https://orcid.org/0000-0002-7687-4471

Nicole Tay
King's College London https://orcid.org/0000-0002-1307-408X

Tobias Banaschewski
Central Institute of Mental Health, Mannheim https://orcid.org/0000-0003-4595-1144

Antoine Grigis

Hugh Garavan
Departments of Psychiatry and Psychology, University of Vermont, 05405 Burlington, Vermont, USA

Andreas Heinz
Charité Universitätsmedizin, Berlin https://orcid.org/0000-0001-5405-9065

Rüdiger Brühl
Physikalisch-Technische Bundesanstalt https://orcid.org/0000-0003-0111-5996

Jean-Luc Martinot
Paris Descartes University https://orcid.org/0000-0002-0136-0388

Marie-Laure Martinot
Institut National de la Santé et de la Recherche Médicale, INSERM U A10 “Trajectoires développementales en psychiatrie”; Université Paris-Saclay, Ecole Norm

Eric Artiges

INSERM/Université Paris-Saclay https://orcid.org/0000-0003-4461-7646
Frauke Nees
Central Institute of Mental Health https://orcid.org/0000-0002-7796-8234
Dimitri Papadopoulos Orfanos
CEA https://orcid.org/0000-0002-1242-8990
Luise Poustka
Department of Child and Adolescent Psychiatry and Psychotherapy, University Medical Centre Gottingen
Sarah Hohmann
Heidelberg University
Juliane Fröhner
Department of Psychiatry and Neuroimaging Center, Technische Universitat Dresden, Dresden, Germany https://orcid.org/0000-0002-8493-6396
Michael Smolka
Technische Universität Dresden https://orcid.org/0000-0001-5398-5569
Nilakshi Vaidya
Henrik Walter
Department of Psychiatry and Psychotherapy CCM, Charite - Universitatsmedizin Berlin, corporate member of Freie Universitat Berlin, Humboldt-Universitat zu Berlin, and Berlin Institute of Health, Be https://orcid.org/0000-0002-9403-6121
Robert Whelan
Trinity College Dublin https://orcid.org/0000-0002-2790-7281
Katarzyna Kalita
Nencki Institute
Haruhiko Bito
Faculty of Medicine, University of Tokyo https://orcid.org/0000-0001-6315-9594
Christian Mueller
University of Erlangen-Nuremberg https://orcid.org/0000-0002-5325-9900
Gunter Schumann
Centre for Population Neuroscience and Precision Medicine (PONS) and SGDP Centre, Institute of Psychiatry, Psychology and Neuroscience, King's College London, London SE5 8AF, United Kingdom https://orcid.org/0000-0002-7740-6469
Hiroyuki Okuno
https://orcid.org/0000-0001-6237-6503

Article

Keywords: alcohol use disorder, amygdala, Arc, cue relapse, alcohol-predicting cue

Posted Date: August 22nd, 2022

DOI: https://doi.org/10.21203/rs.3.rs-1917417/v1

Version of Record: A version of this preprint was published at Molecular Psychiatry on November 10th, 2022. See the published version at https://doi.org/10.1038/s41380-022-01849-4.

Abstract

Alcohol use disorder (AUD) is a chronic and fatal disease. The main impediment of the AUD therapy is a high probability of relapse to alcohol abuse even after prolonged abstinence. The molecular mechanisms of cue-induced relapse are not well established, despite the fact that they may offer new targets for the treatment of AUD. Using a comprehensive animal model of AUD, virally-mediated and amygdala-targeted genetic manipulations by CRISPR/Cas9 technology and ex vivo electrophysiology, we identify a mechanism that selectively controls cue-induced alcohol relapse and AUD symptom severity. This mechanism is based on activity-regulated cytoskeleton-associated protein (Arc)/ARG3.1-dependent plasticity of the amygdala synapses. In humans, we identified single nucleotide polymorphisms in the ARC gene and their methylation predicting not only amygdala size, but also frequency of alcohol use, even at the onset of regular consumption. Targeting Arc during alcohol cue exposure may thus be a selective new mechanism for relapse prevention.

Introduction

Alcohol use disorder (AUD) is a chronic, progressive and relapsing psychiatric disease, with huge costs for afflicted individuals and society, and without effective therapy[1, 2]. Progression of AUD is characterized by periods of abstinence that are followed by alcohol relapses and increasingly longer phases when individuals lose control over alcohol consumption[3–5]. As supported by human studies and animal models alcohol use can be precipitated in abstinent individuals by three main factors that provoke alcohol craving: stress, an alcohol priming dose, or environmental cues that are associated with alcohol availability[5–7]. Thus, in order to develop a successful prevention and therapeutic control of AUD progression the neuronal basis of alcohol craving and relapse must be understood [8, 9].

In neuroanatomical studies, the amygdala has been implicated in the regulation of incentive salience of alcohol- and drug-associated cues, as well as cue-induced reinstatement of drug seeking[10–19]. However, the molecular and genetic mechanisms at play in the amygdala that cause cue-induced relapse have not been identified. In the amygdala, Arc is one of the key molecules regulating plasticity of glutamatergic synapses [20–23]. Arc is engaged in the regulation of α-amino-3-hydroxy5-methyl-isoxazole-4-propionic acid (AMPA) receptor endocytosis[22, 24] and interacts with N-methyl-D-aspartate (NMDA) receptor subunits[25]. As glutamatergic activity is known to regulate alcohol use behavior[26–29], we hypothesized that activity-regulated cytoskeleton-associated protein (Arc)/ARG3.1 might be causally involved in cue-induced relapse.

Using animal model of AUD[30], Arc knockout (Arc^{KO}) murine model, local manipulations of the *Arc* gene in the mouse amygdala with Clustered Regularly Interspaced Short Palindrome Repeats (CRISPR)/Cas9 system[31] delivered by lentiviral vectors, and whole cell patch clamp electrophysiology *ex vivo*, we identified AUD-related behaviors that are regulated by Arc, and Arc-regulated alcohol-induced synaptic plasticity. For translation into humans, we used the IMAGEN cohort database[32] to investigate a possible

association of *ARC* genetic variations with alcohol-related behavioral variables and amygdala volume in young adults at a time when alcohol consumption reaches its peak in life.

Results

Distinct regulation of single AUD-related behaviors by Arc

We trained Arc knockout (Arc^{KO}) mice and their wild-type littermates (Arc^{WT}) to drink alcohol in an IntelliCage social setting[30] (Fig. 1a). The animals went through a training consisting of alcohol introduction (4–20%) and alcohol free access period (FA, 12%). Next, we assessed five behaviors that operationalise DSM-V criteria for AUD[1, 30]: increased motivation to drink alcohol (Motivation, M)[33]; alcohol craving during withdrawal (Withdrawal, W)[34]; reactivity to alcohol-predicting cues (Cue-induced seeking response, CR)[35]; lack of control over alcohol consumption (Alcohol relapse, AR); and persistence in alcohol seeking, even during signaled alcohol non-availability (Persistence, P)[36] (Fig. 1c) (Fig. 1b). An addiction score was calculated as a sum of normalized scores from all AUD tests and an addiction index as a sum of positive results (top 35%) in all tests[30].

Arc^{KO} mice sought significantly more for alcohol during withdrawal and cue-presentation. They showed a higher persistence in alcohol seeking as compared to Arc^{WT} mice and slightly higher motivation to drink alcohol (Fig. 1c). With these behaviors dominating, Arc^{KO} mice reached a higher addiction score and addiction index, than the Arc^{WT} animals (Fig. 1d). We found no significant effect of Arc on novelty seeking or general activity. A lack of Arc did not affect free access alcohol consumption (Fig. 1e) or alcohol consumption during relapse (Fig. 1c). The downregulation of Arc mRNA and protein levels in Arc^{KO} mice, as compared to Arc^{WT} animals, was confirmed by qPCR and western blots from the whole brain homogenates, and by the Arc immunofluorescent staining of the brain sections (Fig. 1f). Altogether, these findings demonstrate a selective role of Arc in AUD-related behaviors, which is confined to alcohol-seeking during alcohol withdrawal and cue presentation.

Alcohol consumption decreases *Arc* gene methylation in the mouse amygdala

To test a causal mechanism of Arc regulation after alcohol drinking, we investigated *ARC* gene methylation and expression in the brain. We trained mice to drink alcohol in the IntelliCages. Mice had free access to 10% alcohol for 45 days and were sacrificed after 6-day alcohol withdrawal. The control alcohol-naïve mice were also trained in the IntelliCages, but never had access to the alcohol (Fig. 2a). The amygdala tissue was used to analyze methylation of 54 CpG sites within *Arc* gene promoter and exon 1 using Targeted NextGen Bisulfite Sequencing (tNGBS) and *Arc* mRNA was assessed by quantitative PCR (qPCR) (Fig. 2b). We found a significant effect of alcohol exposure and interaction between alcohol and CpG site on the frequency of methylation (Fig. 2b). In the mice drinking alcohol the average frequency of

CpGs methylation were significantly decreased both within the *Arc* promoter and exon 1 (Fig. 2c), while the levels of *Arc* mRNA was increased as compared to alcohol-naïve mice (Fig. 2d). Accordingly, we found negative correlations between *Arc* gene expression and methylation frequency of the CpGs in the *Arc* gene promoter and exon 1 (Fig. 2e). There was no significant correlation between alcohol consumption and later *Arc* gene methylation (Fig. 2f). However, *Arc* methylation correlated with alcohol seeking during withdrawal (Fig. 2g). Altogether, these data suggest that previous alcohol consumption and seeking reduced *Arc* gene methylation in the amygdala, which enhanced Arc mRNA expression.

Arc mRNA expression is increased in the amygdala of the mice with AUD-resistant phenotype

To test a link between Arc mRNA expression and AUD-prone phenotype, we investigated transcriptome in the amygdala of the mice trained to drink alcohol in the IntelliCages and diagnosed as AUD-prone (Addiction index ≥ 2) or resistant (Addiction index < 2) [37] (Fig. 2h). Addiction-prone and resistant mice differed in addiction score, activity as well as AUD behaviours (Fig. 2i-j). The amygdala tissue was collected and total RNA extracted. There were higher levels of Arc mRNA in the amygdala of AUD-resistant mice as compared to AUD-prone drinkers (Fig. 2k), suggesting that Arc mRNA expression has protective effects during AUD progression.

Arc protein is recruited in the mouse amygdala during cue-induced alcohol seeking, but not during drinking

In order to further test this specific role of Arc protein in distinct AUD-related behaviors, C57BL/6J mice were trained in IntelliCages and sacrificed during period of free access to alcohol (FA, day 95), after alcohol withdrawal (W, day 101), or after 90 min of cue (light)-induced alcohol seeking (CR, day 101). Control animals were also trained in the IntelliCages, but never had access to alcohol, and were sacrificed during the FA phase (day 95) (Fig. 3a). We observed that the alcohol-naïve and alcohol drinking mice did not differ in general activity (Fig. 3b). Previously alcohol drinking mice showed alcohol-seeking behavior, when the alcohol was abandoned. As expected, this behavior decreased during withdrawal (FA vs. W), indicating the beginning of extinction of alcohol seeking behavior when the reward corner was inactive (Fig. 3b). However, they increased alcohol seeking during cue presentation, as compared to the last day of the withdrawal (W vs CR), indicating a cued recall of the alcohol reward memories (Fig. 3b). Brains were sliced and immunostained to detect Arc and PSD-95, as a marker of the glutamatergic synapse[38]. Arc expression was analyzed in the central (CeA) and basolateral nuclei of the amygdala (BLA) (Fig. 3a). We focused on these nuclei as previous work linked them with multiple addiction-related behaviors, including craving and cue-induced reinstatement of alcohol seeking[10–18]. Arc protein was detected as immuno-positive puncta (Arc^+) that often colocalized with PSD-95-positive puncta ($PSD\text{-}95^+$), indicating their location at excitatory synapses (Fig. 3c-d). We found no effect of the alcohol drinking on Arc levels, but a significant upregulation of the Arc protein levels after cue-induced seeking. Similar changes of Arc expression were observed in BLA, however, they did not reach statistical significance (Fig. 3e). Thus,

overall our data indicate that increased Arc mRNA expression during alcohol withdrawal enables increased Arc protein levels during cue relapse. We also observed a dissociation of Arc protein upregulation in the CeA between cue-induced alcohol seeking, withdrawal-associated alcohol seeking and alcohol drinking.

Motivation to drink alcohol and relapse induced by alcohol-predicting cues are regulated by CeA Arc

As we identified the CeA as a crucial brain region where Arc activity is associated with cue-induced alcohol seeking, we causally probed this relationship. To this end, we developed a CRISPR/Cas9 system for local *Arc* gene manipulation *in vivo* using plentiCRISPRv2 plasmids[39]. First, five *Arc* gene-specific guide RNAs (gRNAs) were designed and tested *in vitro* (**Supplemental Fig. 1a**). gRNAs, cloned into plentiCRISPRv2, significantly downregulated Arc protein expression in stimulated mouse dissociated neuronal culture (**Supplemental Fig. 1b-c**). As gRNA1 is located at the beginning of the *Arc* gene coding sequence, plentiCRISPRv2 with gRNA1, and plentiCRISPRv2 without gRNA, were used to produce lentiviral vectors (Arc^{Crispr} and empty vector, EV). After transduction of mouse neuronal culture with Arc^{Crispr} sixteen specific indel mutations were identified within the gRNA complementary sequence of *Arc* gene (**Supplemental Fig. 1d**), confirming specificity of the mutation. None of such mutations were found in the EV neurons. Arc^{Crispr} stereotactically delivered to CeA transduced the cells with 60% efficiency and 96% specificity for neurons (Supplemental Fig. 2). We found that a local downregulation of Arc reduced the AMPA/NMDA EPSCs ratio in CeA neurons (**Supplemental Fig. 2**), and prevented Arc protein expression in CA1 after PTZ kindling (**Supplemental Fig. 3**) in the adult mouse brain.

Mice were bilaterally injected into the medial part of CeA (CeM) with Arc^{Crispr} or EV. We focused on CeM since it was previously linked with reward and reward-associated cues [11–14]. The animals underwent long-term alcohol training in the IntelliCages (Fig. 4a-b). During cue-induced alcohol seeking, Arc^{Crispr} mice made significantly more nose pokes to the alcohol corner than the EV animals (Fig. 4c). Arc^{Crispr} mice also reached a higher breakpoint during the motivation test, as compared to EV mice. There were no significant differences between the Arc^{Crispr} and EV mice in alcohol seeking during alcohol withdrawal, alcohol consumption during alcohol relapse and performance during a persistence test (Fig. 4c). The mice from two experimental groups did not differ in general activity and alcohol consumption during the introduction phase and FA periods in the Intellicages (**Supplemental Fig. 4a-b**). The post-training analysis of the brain sections confirmed that Arc^{Crispr} and EV were expressed mostly in the CeM (**Supplemental Fig. 4c**) and Arc^{Crispr} mice had significantly reduced levels of total and synaptic Arc in CeM, as compared to the EV mice (**Supplemental Fig. 4d**). Thus, the CeM Arc specifically controls motivation to drink alcohol and alcohol seeking during relapse induced by alcohol-predicting cues. These findings suggest a causal role of Arc in the CeM for the control of cue-induced alcohol seeking.

CeA Arc does not regulate sucrose seeking

Since our data indicates that Arc expression in the CeM controls alcohol motivation and seeking during cue-induced alcohol seeking (Fig. 4c), in the next step we tested whether this effect was specific for alcohol-predicting cues or affecting cues associated with other rewards as well. A naïve cohort of mice underwent stereotactic surgery. Arc^{Crispr} and EV were bilaterally injected into CeM and the mice underwent long-term training in the IntelliCages. The training resembled the alcohol training, however, this time 5% sucrose was used as a reward (**Supplemental Fig. 5a-c**). Arc^{Crispr} mice did not differ from the EV group, as far as visits in new corners, general activity and sucrose consumption were concerned (**Supplemental Fig. 5d**), indicating no effect of Arc^{Crispr} on novelty and reward seeking traits that are associated with propensity for AUD[30, 40]. We also did not find any effect of Arc^{Crispr} on addiction-related behaviors in the mice trained to drink sucrose (**Supplemental Fig. 5e**). These findings suggest no role of CeM Arc in cue-induced seeking of natural rewards.

Arc regulates alcohol-induced synaptic plasticity in CeM

After showing a specific role of Arc in cue-induced alcohol seeking behavior, we asked whether Arc affects plasticity in this process. As Arc regulates internalization of AMPA-R[22, 23], we hypothesized that Arc regulates the function of CeM synapses during cue-induced alcohol seeking. We trained Arc^{KO} and Arc^{WT} mice to drink alcohol or water. Thereafter, they were sacrificed, either after alcohol withdrawal or after 90 min of cue-induced alcohol seeking. As a control, alcohol-naïve water drinking mice were used (Fig. 5a). We performed whole-cell voltage clamp recordings from the neurons of the CeM while stimulating axons from BLA (Fig. 5b), and measured the ratio of AMPA-R and NMDA-R excitatory postsynaptic currents (EPSCs). We focused on this projection as former data showed that the BLA-CeM pathway can drive appetitive behaviors[41, 42]. We found that the AMPA/NMDA ratio was lower in Arc^{KO} as compared to Arc^{WT} mice when only drinking water. Cue-induced alcohol seeking coincided with a decrease in the AMPA/NMDA EPSCs ratio in the Arc^{WT} mice compared to the withdrawal condition suggesting a weakening of synaptic transmission. The opposite changes were observed in Arc^{KO} mice. The AMPA/NMDA ratio was significantly upregulated during cue-induced alcohol seeking, as compared to the withdrawal condition (Fig. 5c). These findings suggest that Arc is required for the plasticity of BLA-CeM synapses during presentation of alcohol-predicting cues when the cues are not accompanied by alcohol reward. Thereby, the CeM Arc would appear as a signal that updates the incentive value of an alcohol cue. Every cue-induced retrieval of the alcohol seeking behavior is at the same time an extinction trial. If not eventually followed by the reward (alcohol), it would weaken the cue-alcohol association, and eventually lead to an extinction of seeking behavior.

ARC genetic variations are associated with alcohol consumption in humans

To check the contribution of the human *ARC* gene to the expression of alcohol addiction-related behaviors at a time point when they get established, we interrogated the IMAGEN sample of 1315 19-year

old participants[32], controlling for gender and site of data collection (Fig. 6, **Supplemental Table 1**). We found a significant effect of the single nucleotide polymorphism (SNP) rs10097505 (variant: G > A) and the methylation of 15 CpG sites on the amount of consumed alcoholic beverages over 12 months. Thereby, the individuals with the AA variant tended to drink more alcohol than those with GG and GA (Fig. 6a, **Supplemental Table 2**).

Since alcohol consumption may induce DNA hypomethylation[43] (Fig. 3), we investigated blood DNA methylation in the IMAGEN cohort using the Illumina 850K BeadChip array. The CpG sites analysis demonstrated that the frequency of drunkenness positively correlates with methylation of cg05415840 and the amount of consumed alcohol positively correlates with cg08387463 methylation within exon 1. However, binge drinking frequency negatively correlated with methylation levels of cg04321580 and cg19438565 located within the *ARC* promoter (Fig. 6a, **Supplemental Table 3**). Moreover, to investigate whether methylation was genotype-dependent, correlations between the methylation of four CpG sites (cg08387463, cg04321580, cg19438565, cg05415840) and the SNP rs10097505 variant were computed (**Supplemental Table 3**). The analysis revealed that the cg19438565 and cg05415840 methylations were significantly correlated with the variable rs10097505, suggesting that those two CpG sites were genotype-dependent (Fig. 6a, **Supplemental Table 3**. To test whether the SNP variants influence methylation levels and its association with alcohol consumption, Pearson's correlation test was conducted between the ESPAD variables and two CpG sites, controlling for the genotype (rs10097505) in addition to cells, gender, wave, and sites. The test revealed a significant association between cg19438565 and frequency of binge drinking (**Supplemental Table 4**). The loss of the previously significant correlation between the frequency of drinking and cg05415840 after controlling for the genotype could be due to the methylation mechanisms being driven by the genotype. On the other hand, the fact that the correlation between binge drinking and cg19438565 did not change substantially, indicates that the tested variables are not influenced by the variation in the genotype, suggesting the environmental effect that modulates this CpG site. Altogether, the findings show that natural variation in the Arc gene and its methylation levels influence key AUD-related behaviors – amount and frequency of alcohol consumption – that are known to be alcohol cue-controlled.

ARC gene methylation predicts amygdala volume in humans

Next, we tested the correlation between the methylation at three CpG sites (cg08387463, cg04321580, cg19438565; excluding cg05415840 since the results showed that the methylation at this CpG site is driven by the genotype) with the amygdala and hippocampus volumes at both hemispheres. Pearson's correlation analysis was conducted controlling for gender, site, cells, wave and total intracranial volume (Fig. 6b). This analysis showed a negative correlation of the left amygdala with the cg08387463 CpG methylation levels (Fig. 6b**)**. The result of the analysis indicates that the methylation at the *ARC* cg08387463 CpG site is linked to the left amygdala volume (**Supplemental Table 5**).

Discussion

AUD is a common psychiatric disorder with no effective pharmaco-treatment available to interfere with maladaptive behaviors. At the core of this disorder, and criterion for AUD diagnosis, is the uncontrollable cued relapse to alcohol taking after established periods of abstinence. Here we propose a new mechanism how cue-induced alcohol seeking behavior is regulated, which dissociates from mechanisms controlling alcohol consumption per se. The amygdala protein Arc is exclusively enhanced during cue-induced alcohol seeking. Its activity in the CeM determines cue-induced alcohol seeking, but shows no role in later alcohol drinking behavior. As such, it mediates the starting point of a cued relapse episode, but not its end. As Arc is essential for synaptic plasticity of the BLA-CeM projection, it is suggested that Arc in the CeM is recruited for an update of the cue incentive properties and thereby an essential regulator of addiction memory. This conclusion is in line with earlier reports showing that CeA activity is regulated by alcohol cues, as well as with the CeA regulating incentive salience of drug-associated cues[11, 12] and reinstatement of drug seeking by cues associated with drug reward[15–18]. Long-term alcohol consumption affects glutamatergic transmission within the mesocorticolimbic system that ultimately controls drug reward and reinforcement, as well as drug craving and seeking[44–46]. Significant changes of AMPA-R and NMDA-R currents, and frequency of silent synapses that lack functional AMPA receptors, were observed after long-term alcohol consumption, alcohol withdrawal, relapse and presentation of alcohol-associated cues in multiple brain regions including the amygdala[10, 37, 47–49]. In human patients, the genetic variation in the NMDA-R dependent AMPA-R trafficking cascade is associated with alcohol dependence[49, 50]. However, the molecular processes that drive the alcohol-induced modifications of the glutamatergic synapses and AUD-related behaviors are only beginning to be elucidated[9].

Here, we found that Arc^{KO} mice had an overall higher addiction index, as compared to Arc^{WT} mice (Fig. 1). This phenotype was a consequence of increased alcohol seeking during withdrawal and relapse induced by alcohol-predicting cues, increased persistence in alcohol seeking and a tendency to display higher motivation for alcohol, but without effects on alcohol consumption. A local knockdown of Arc in CeM confirmed this phenotype in cue relapse and motivation test (Fig. 3). Moreover, we observed higher Arc mRNA levels in the amygdala of the mice diagnosed as AUD-resistant, as compared to AUD-prone individuals. Thus, Arc expression is a protective factor for several AUD-related behaviors. This conclusion is in concordance with earlier studies demonstrating decreased *Arc* mRNA levels in the amygdala of early onset alcoholics[51].

Although Arc protein expression is induced in neurons by multiple stimuli[52], only a few studies showed a causal link between Arc expression and animal behavior. In particular, Arc affects memory formation, cognitive flexibility, anxiety, cocaine self-administration and schizophrenia-related behaviors[22, 53–57]. Decreased Arc expression in the amygdala was implicated in increased early life stress-induced alcohol consumption in animal models [51, 53, 58]. In human studies, a correlation between *ARC* gene polymorphism was confirmed solely for schizophrenia and Alzheimer's disease[59, 60] so far. Here, we show for the first time a link between *ARC* gene variation and alcohol consumption in the IMAGEN cohort

of young adults. *ARC* gene rs10097505 SNP affects the amount of consumed alcohol (Fig. 5). The individuals with the AA variant drink more alcohol, then people with GA or GG variants (**Supplementary Table 2**). Since the AA variant confers also a risk factor for Alzheimer's disease, and these patients have lower levels of ARC mRNA in the cortex as compared to healthy controls[60], our findings suggest that individuals with higher alcohol consumption, which can be seen as the natural result of enhanced occurrence of cue-induced relapse episodes, have lower *ARC* expression. This is in agreement with the study showing that AUD patients have less ARC mRNA in the amygdala[51]. Moreover, methylation of the *ARC* promoter (cg04321580 and cg19438565) negatively correlates with frequency of binge drinking, while cg08387463 methylation within exon 1 positively correlates with alcohol consumption. In agreement with previous study[61], increased methylation in the Arc gene body is predictive of lower *ARC* expression associated with higher and more frequent alcohol consumption.

An important limitation of this finding is that the analysis was conducted in blood samples. Therefore, it is uncertain whether a similar pattern of methylation is observed in the brain and whether it affects Arc expression in the same way. Nevertheless, as we observed that high cg08387463 methylation predicts not only high alcohol consumption, but also low left amygdala volume in the IMAGEN cohort (Fig. 6b), methylation of cg08387463 may be a potential blood marker of alcohol use. Importantly, in concordance with previous studies lower amygdala volume is a risk factor for heavy alcohol drinking in young adults[62–64].

We therefore propose Arc in the amygdala as a unique regulator for cue-induced alcohol seeking which drives relapse to alcohol drinking behavior as part of an AUD. Arc appears to be essential for concurrent updating of the cue incentive salience. Its time-dependent selective pharmacological targeting at cue exposure may therefore offer a new therapeutic strategy for one of the key AUD associated behaviors.

Materials And Methods

Subjects. C57BL/6J mice were purchased from the Medical University of Bialystok, Poland. Arc^{KO} mice were obtained from Dr. Hiroyuki Okuno (Kagoshima University, Kagoshima, Japan) and bred as heterozygotes at Nencki Institute. Mice were 10-week old at the beginning of the experiments. Animals were housed under a 12/12 hr light/dark cycle in standard mouse home cages with *ad libitum* access to water and food. Experiments were approved by the Animal Protection Act of Poland guidelines and the 1st Local Ethical Committee in Warsaw, Poland (no. 117/2016). All experiments were planned to reduce the number of animals used and to minimize their suffering.

Arc/ARG3.1 knockout mice. Arc^{KO} mice were generated by the homologous recombination with integration of the targeting vector into the *Arc* gene locus (strain: C57BL/6N) at Kenji Sakimura lab, Niigata University, and Haruhiko Bito lab, the University of Tokyo (H.O. and H.B.). The *Arc* gene-targeting was confirmed by Southern blotting, targeted genomic sequencing, Western blotting, and RT-PCR. Genotypes were identified by PCR using tail DNA with the following specific primers: For Arc^{KO}: Forward,

5’- cgtcgggccactttgtacaag -3’, Reverse, 5’- tgtagagggtgaggccaatg -3’ and for Arc^{WT}: Forward, 5’- agaggagttcttagcctgttcgg -3’, Reverse, 5’- tctcctggcagcggcaaagacagg -3’.

qPCR for Arc mRNA. The amygdala of Arc^{WT} and Arc^{KO} mice was quickly dissected on ice from the fresh brain, homogenized and stored in RNAlater solution (Invitrogen, AM7020) at 4°C for 24 hours and then kept at -20°C till further use. Total RNA was extracted using the RNeasy Mini kit (Qiagen, 74104) according to the manufacturer’s recommendations. RNA concentration, quality and integrity were determined using a Nanodrop 1000 (Thermo Scientific) and a Bioanalyzer (Agilent). QuantiTect Reverse Transcription Kit (Qiagen, Cat. No. 205314) was used to quickly prepare gDNA for gene expression analysis. *Arc* was quantified by using the QuantiFast SYBR® Green PCR Kit (Qiagen, Cat No. 204054). The recommended cycling program from this kit was followed for the amplification. *Arc* primer was bought from Qiagen (QuantiTect Primer Assay, *Arc*: QT00250684). As a control, Gusb expression was analyzed; the Gusb primer was also bought from Qiagen (QuantiTect Primer Assay, Gusb: QT00176715). The amplification was conducted with the Step One Plus real-time system (Applied Biosystem). To analyze the fold *Arc* expression the delta-delta Ct method was used [65].

IntelliCage Behavioral Training. Female mice were trained for long-term alcohol drinking in the IntelliCage System (NewBehavior; https://www.tse-systems.com/) based on a previously established protocol [30]. Animals were briefly anesthetized by isoflurane and subcutaneously injected with RFID transponder tags which allow for their identification in the IntelliCage corners. Mice underwent a week of cage adaptation to habituate to the light/dark cycle and cage conditions. During the cage adaptation period (d1-7) mice had unlimited access to the corners, food and water in the corners. The novelty seeking behavior was used as an anxiety-related trait [30]. The number of exploratory visits to the corners was measured during the first hour of the cage adaptation. Next, mice underwent a nosepoke adaptation (d3-7) under a fixed ratio of reinforcement (FR 1), when each nosepoke in the corner was rewarded by 5-second access to water. When all animals learned how to reach the bottles inside the corners, a free alcohol access period started (d7-47) with alcohol in increasing concentrations (4, 8, 12, 16, 20%, 3 days each) and 12% during the rest of the training. Alcohol availability was signaled by the cue light presented each time a mouse entered the corner. Each time when a mouse entered the alcohol corner a cue-light was on, serving as an alcohol-predicting cue. Each nosepoke to the alcohol corner gave access to alcohol for 5 s. Daily alcohol consumption (g/ kg/ day) was calculated with the formula:

Number of licks of alcohol per day x lick volume (1.94 µl) x % alcohol x 1 g/ ml) / mouse weight

AUD-related behaviors (d47-97). During *a motivation test* (d47-53) mice were subjected to an increasing fixed-ratio (FR) schedule to have access to the reward corner. Mice had to perform an increasing number of nosepokes during a visit to the reward corner to have access for 5 seconds to the bottles. The number of required nosepokes increased (2, 4, 8, 12, 16, 20 …) when a mouse repeated the task 10 times. The FR level reached by a mouse during the test was used as an index of motivation. During the *withdrawal test* (d60-66) the reward corner was inactive. During this period the cue-light associated with the alcohol was off and no alcohol was available. Alcohol seeking was calculated as an average daily number of

nosepokes to an alcohol corner. The test was followed by *a cue-induced relapse* (d66) during which the alcohol-predicting cue light was presented, but no alcohol was available. Relapse was assessed as a number of nosepokes to an alcohol corner during the first 6 hours of the test. During *the alcohol relapse* (d67) mice had full access to the reward corner: the cue-light was on and alcohol was present. Alcohol relapse was measured as the amount of consumed alcohol (g/kg/day). *The persistence test* (d68-71) was divided into two phases, changed every 6 hours. The active phase (A) - mice had access to alcohol signaled by the cue light. During the non-active phase (nA), mice had no access to alcohol. Persistence was calculated as a change of nosepokes number to alcohol corner during nA as compared to A (nA-A).

To calculate *Addiction index* mice performance in all tests was assessed. Mice were labeled as positive in a test if they performed in the top 30% of the population. Addicted drinkers were positive in at least two tests. Non-addict drinkers were positive maximum in one test. To calculate the individual *Addiction score* each scores for all tests were normalized and summed up according to the formula: *AS = Σ(Vi (individual score)−mean(population))/SD(population)*

Western blot. The hippocampus and amygdala of Arc^{WT} and Arc^{KO} mice were quickly dissected on ice from the fresh brain. Tissue was collected in the RIPA lysis buffer (Santa Cruz, sc-24948). After centrifugation the supernatant was stored at -80 °C until further analysis. Equal amounts of protein lysate were mixed with the Laemmli buffer and left to denature at 70 °C for 10 minutes. The mixture was loaded on precast gel wells (Bio-Rad, #4568083). The membranes were blocked by 5% milk diluted in TBST (Tris-buffered saline with Tween 20), and incubated with anti-Arc antibody at 1:1000 overnight (o/n) (SYSY156 003; RRID: AB_887694). Anti-Gapdh at 1:50000 o/n (Millipore, MAB374; RRID:AB_2107445) was used as internal control for normalization. The membrane was washed in TBST and incubated with the horseradish peroxidase (HRP) secondary antibodies at 1:5000 (anti-rabbit IgG-HRP, Santa cruz, sc-2030, RRID:AB_631747; mouse-IgGκ BP-HRP, Santa cruz, sc-516102, RRID:AB_2687626). The membrane was visualized by G-Box apparatus using chemiluminescent reagent (Advansta, K-12042-D10).

Immunostaining. Mice were transcardially perfused with PBS and 4% PFA/PBS. The 40 µm-thick brains sections were cut on a cryostat (Leica, CM1950) and processed for immunostaining. The brain slices were washed 3 6 minutes in phosphate-buffered saline (PBS). Next, the sections were blocked with a blocking solution (5% NDS /Triton 0.3% /PBS) for 1 hour at room temperature (RT). Then, the slices were incubated with the 1^{st} antibody solution overnight (o/n) (Anti-Arc (SYSY156 003; RRID: AB_887694) 3 days 1:1000; Anti-PSD95 (Millipore MAB1598, RRID: AB_94278), 1:500; Anti-NEUN, (Abcam, ab177487; RRID:AB_2532109), 1:300; Anti-Flag (Novus, NBP1-06712ss; RRID:AB_1625982), 1:1000; Anti-Flag (Abcam, ab95045; RRID:AB_10676074), 0.5 µg/ul. The next day, the slices were washed 3 6 minutes in PBS with 0.3% Triton. After the washing, the secondary antibody (AlexaFluor 488, Donkey Anti-rabbit IgG(H+L) Thermofisher #A-21206 (RRID:AB_2535792), 1:500; AlexaFluor568, Donkey Anti-rabbit IgG(H+L), Thermofisher #A10042 (RRID:AB_2534017), 1:500) was applied for 1.5 hour at RT. Next, the slices were washed 3 6 minutes in PBS, mounted on microscope slides and covered with coverslips using Fluoromount-G with DAPI (Invitrogen 00-4959-52).

Immunostaining analysis. The staining was analyzed by SP8 confocal microscope (Leica) using the 63 X objective with 1.66 increasing zoom. Single scan was taken into the analyzed brain structures with a resolution of 148.36 µm x 148.36 µm. Six to eight microphotographs were taken per animal, from every sixth section through the dorsal hippocampus and amygdala. The mean gray value of the images (arbitrary units), density and size of Arc+ puncta were analyzed by ImageJ (1.48v) software while the data analysis was performed using scripts in Python (3.4.4v). Hippocampal dissociated cell culture immunostaining was analyzed by All-in-One Fluorescence Microscope BZ-X800 (Keyence) using the 20 X objective. For each transfected neuron the mean gray value was analyzed by ImageJ (1.48v) software.

Arc gene methylation in mice. The amygdala of alcohol-naïve and alcohol trained C57BL/6J mice was quickly dissected on ice. Samples were immediately frozen in liquid nitrogen. Genomic DNA was extracted by Extractme genomic DNA Kit (Blirt, EM13) following the suggested protocol. DNA was analyzed by EpigenDx (96 South Street Hopkinton, MA 01748, www.epigendx.com) for methylation analysis by Targeted NextGen Bisulfite Sequencing (tNGBS).

Arc KO generation using CRISPR/Cas9 system. The 20-bp sequences directly upstream of 5'-NGG sequences (PAM sequences) in the coding region of *Arc* gene were identified (Supplemental Materials and Methods). Four sequences with the lowest probability of off-targets and high on-target efficiency were chosen. LentiCRISPR v2 plasmids expressing the CRISPR/Cas9 system with Flag-tag[39] or GFP reporter protein were used (Addgene plasmid #52961; RRID: Addgene_52961; plasmid #82416; RRID: Addgene_82416).

To clone the gRNA into the lentiCRISPR vectors, the cloning protocol of Zhang Lab was used (media.addgene.org/data/plasmids/52/52961/52961-attachment_B3xTwla0bkYD.pdf). Efficiency and specificity of mutation was validated *in vitro* and *in vivo.* Five gRNAs for *Arc* coding sequence were designed and tested to check the efficacy in the depletion of Arc protein expression. gRNA1-2 were designed using http://crispr.dbcls.jp/, gRNA3-4 using https://chopchop.cbu.uib.no/, gRNA5 is from GenScript (cat. SC1678). gRNAs were cloned into plentiCRISPRv2_Flag [39]. The same plasmids without gRNA (empty vector, EV) were used as a control for *in vivo* experiments. The plasmids were used to generate lentiviral vectors (LV), Arc^{Crispr} and EV, at Nencki Institute core facility Animal Models lab. For *in vitro* studies, as Flag control plasmid (Ctrl), the Flag tagged KASH fragment [66] was subcloned into the pcDNA3 vector, resulting in the pcDNA3-5x Flag-KASH (Thermo Fisher). As GFP control (Ctrl), a monomeric version of EGFP was subcloned into a CAG promoter vector to make pCAG-mEGFP.

Validation of CRISPR/Cas9 system in vitro. The plasmids expressing gRNAs 1-5 were tested in the mouse hippocampal dissociated cell culture. Neurons were transfected with lipofectamine 2000 (Invitrogen, cat. 11668-027) on the 10^{th} day *in vitro* (DIV) and after 4 days, tetrodotoxin (TTX, 2 µM, Tocris, Cat. No. 1078) was added to the medium to block neuronal activity. After one day, cells were stimulated with bicuculline cocktail (bicuculline 30 µM (Tocris, Cat. No. 0109), 4AP 100 µM (Sigma-Aldrich, Cat. No. 275875), glycine 100 µM (Sigma-Aldrich, Cat. No. 50046), strychnine 1 µM (Sigma-Aldrich, Cat. No. S0532) to disinhibit cells and induce Arc protein expression. After the 3-hour stimulation, cells were fixed in 4% PFA and

immunostained to detect Arc protein and GFP/Flag reporters. The *in vitro* experiments were replicated three times.To confirm the mutation of the *Arc* gene by CRISPR/Cas9 system with gRNA1, mouse cortical dissociated cell culture was transduced on DIV5 with LVs coding plentiCRISPRv2 with GFP and gRNA1 (LentiCRISPRv2GFP, plasmid #82416, Addgene). After 2 weeks, the cells were lysed and genomic DNA extracted by Extractme genomic DNA Kit (Blirt, EM13). DNA was used for PCR amplification of the *Arc* gene with a set of primers specific for the region containing the sequence complementary to gRNA1 (primer forward: 5'ctctgggcctctctagcttc3', primer reverse: 5'cgtccaagttgttctccagc3'). The same procedure was applied to non-transduced cells to obtain non-mutated genomic DNA. The amplicon was sent for Sanger sequencing by Genomed S.A. (Warsaw, Poland). The chromatograms were analyzed with the ICE (Synthego) program which gives NGS quality results with Sanger data.

Validation of CRISPR/Cas9 system in vivo. Three weeks after CA1-targeted, bilateral, stereotactic injection of LV coding EV or Arc^{Crispr} (900 nl, 10^7-10^8 GC/ µl) mice received i.p. injections of pentylenetetrazol (PTZ, Sigma P6500) to induce Arc expression (d1: 3 10 mg/kg or saline, every 30 minutes; d2: 3 30 mg/kg or saline, every 30 minutes). Mice were sacrificed and perfused 2 hours after the last injection if they developed seizures. Brain slices were used to assess Arc protein levels and LV expression.

Electrophysiology. The experiments were performed on female and male adult C57BL/6J and Arc KO mice and their wild type (WT) siblings. Mice were 1-2 months old at the beginning of the behavioral paradigm and 3-4 months old at the time of electrophysiological recordings. Mice were housed separately in their home cages, receiving food and water *ad libitum.* Mice exposed to long-term alcohol protocol received an additional bottle containing alcohol solution in drinking water. Alcohol was prepared as a solution of 96% ethanol and tap water. The concentration of ethanol in water increased from 4% during the first four days of exposure, to 8% for the remaining 30 days. The alcohol consumption (as well as normal water) was measured every 2 days.

Whole-cell patch-clamp technique was used to analyze AMPA/NMDA EPSCs ratio. Brains from decapitated mice were quickly submerged in the ice-cold cutting solution (135 mM NMDG, 1 mM KCl, 1.2 mM KH_2PO_4, 1.5 mM $MgCl_2$, 0.5 mM $CaCl_2$, 20 mM choline bicarbonate, 10 mM D-glucose, bubbled with carbogene – 5% CO_2, 95% O_2). Coronal 250 µm-thick slices were prepared using Leica VTS1000 vibratome. Slices containing the amygdala were collected into a chamber filled with artificial cerebrospinal fluid (ACSF,119 mM NaCl, 2.5 mM KCl, 1 mM NaH_2PO_4, 26 mM $NaHCO_3$, 1.3 mM $MgCl_2$, 2.5 mM $CaCl_2$, 10 mM D-glucose, bubbled with carbogene) and incubated for at least 60 min at room temperature. Slices were then transferred to the recording chamber, perfused with ACSF solution heated up to 31°C. The stimulating electrode was placed in the axons from the basal amygdala. CeM neurons were identified visually and patched with borosilicate glass capillaries (3–6 MΩ resistance) filled with internal solution (130 mM Cs gluconate, 20 mM HEPES, 3 mM TEA-Cl, 0.4 mM EGTA, 4 mM Na_2ATP, 0.3 mM NaGTP, and 4 mM QX-314Cl, pH = 7.0–7.1, osmolarity: 290–295 mOsm). Series and input resistances were monitored throughout the experiment. Electrical stimulation was elicited by TTL pulse every 5 s. Recorded currents were filtered at 2 kHz (npi amplifiers) and digitized at 10 kHz (ITC-18

InstruTECH/HEKA). All recordings were performed in the presence of 50 µM picrotoxin (Abcam) in ACSF, to pharmacologically block inhibitory neurotransmission and focus on the excitatory pathway specifically. After reaching the whole-cell configuration, baseline currents were recorded for 2-3 minutes to ensure the stability of recorded amplitudes. *AMPA/NMDA EPSCs Ratio.* To measure the AMPA/NMDA ratio, 50-100 stable sweeps were recorded at -60 mV and +45 mV for AMPA and NMDA EPSCs, respectively, and their peak amplitudes were averaged. Since the EPSC recorded at +45mV is a composite of AMPA-R- and NMDA-R-mediated current, the amplitude of NMDA response was measured 50 ms after the peak to ensure the absence of the AMPA-R component. All electrophysiological recordings were performed by the experimenter blinded to the mouse genotype. For the analysis of recordings, we averaged the data from multiple cells of one animal, thus showing the overall effect of alcohol on an individual mouse. The number of recorded cells from each experimental group are indicated in the figure legend.

Stereotactic Injection of viral vectors. The surgeries were performed at least 7 days before the beginning of the training. Lentiviruses for the CRISPR/Cas9 system with the gRNA1 or the corresponding empty vector were produced at Animal Models Lab at Nencki Institute (Warsaw, PL). Lentivirus (LV) solution (alcohol and sucrose experiment: 200 nl, 10^7-10^8 GC/ µl; electrophysiology experiment: 900 nl, 10^7-10^8 GC/ µl) was injected into the CeA (Bregma AP -0.12, ML $^+/_-$ 0.28, DV -0.46) (Paxinos and Franklin, 2008) at the rate of 0.1 µl per minute through the beveled, 26-gauge metal needle and 10 µl microsyringe (SGE010RNS, WPI, USA). The needle was removed from the brain ten minutes after the injection to prevent outflow.

IMAGEN study. Samples were drawn from the IMAGEN cohort, a European multi-center imaging-genetics study of adolescents recruited and tested across eight assessment sites (London, Nottingham, Dublin, Mannheim, Berlin, Hamburg, Paris, and Dresden). The recruitment process, exclusion and inclusion criteria and the procedure have been described elsewhere [67]. From the IMAGEN cohort, data were only included if behavioral, genetic, methylation and MRI data were available. After quality control and removal of outliers, a sample of 1315 19-years-old participants (52.8% females) was used for statistical analysis. Local ethics research committees at each IMAGEN site permitted the study. Alcohol-related behaviors were measured using the European School Survey Project on Alcohol and Drugs (ESPAD) questionnaire with the focus on the self-reported quantity of consumed substance, frequency of drunkenness, and binge drinking over the last 12 months.

Structural MRI data were acquired with 3T magnetic resonance (MRI) scanners (Siemens, GE and Philips). The same scanning protocols were applied across all IMAGEN sites. Full details of MRI acquisition protocols and quality checks have been previously described [68]. FreeSurfer software suite (http://surfer.nmr.mgh.harvard.edu/) was utilized to segment MRI brain images and inspect each individual cortex for inaccuracies. Participants with cerebral cortex malformations were excluded from analyses. For this study, values referring to the total volume of four brain regions: Left Amygdala, Left Hippocampus, Right Amygdala, Right Hippocampus, were extracted. Since IMAGEN data was collected at

8 different sites, the effect of site was added as a nuisance covariate in all statistical analyses in addition to total intracranial volume [32].

The tested variables in the *European School Survey Project on Alcohol and Drugs (ESPAD) questionnaire* were: 8b - On how many occasions over the last 12 months have you been drunk from drinking alcoholic beverages? - Based on a scale from 0 to 6, where 0 = '0', 1 = '1–2' times; 3 = '6–9', 4 = '10-19', 5 = '20-39', and 6 = '40 or more' times. 17b - 'On how many occasions over the last 12 months have you had any alcoholic beverage to drink?' - Based on a scale from 0 to 5, where 0 = '0', 1 = '1', 2 = '2', 3 = '3-5', 4 = '6-9', and 5 ='10 or more' times. 19b - How many times over the last 12 months have you had five or more drinks in a row?'. - Based on a scale from 0 to 6, where 0 = '0', 1 = '1–2' times; 3 = '6–9', 4 = '10-19', 5 = '20-39', and 6 = '40 or more' times.

Omics Data. DNA was extracted from whole-blood samples. DNA purification and genotyping took place at the Centre National de Génotypage in Paris. The whole blood samples (∼10mL) were collected from participants at the age of 14 and retained in BD Vacutainer EDTA tubes (Becton, Dickinson & Company) utilizing the Gentra Puregene Blood Kit (QIAGEN) in line with the instructions specified by the manufacturer.

Genotype data were obtained for 582,982 markers utilizing DNA extracted from whole blood and the Illumina (Little Chesterford, UK) HumanHap610 Genotyping BeadChip. SNPs with call values of <98%, minor allele rate <1% or variation from the Hardy-Weinberg equilibrium ($P \leq 1\times10^{-4}$) were rejected from further examinations. Subjects with an unclear sex code, absent genotypes (failure rate >2%), and outlying heterozygosity (with a frequency of 3 SD from the Mean) were also removed. The identity-by-state resemblance was employed to assess cryptic relatedness for individuals with the PLINK program. Individuals who were closely related to identity-by-descent (IBD > 0.1875) were excluded from the subsequent analysis. The population was investigated using principal component analysis (PCA) in EIGENSTRAT software. The four HapMap populations were managed as reference groups in the PCA and participants with atypical ancestry were also eliminated. Genotype data were coded into minor homozygotes, heterozygotes, and major homozygotes.

ARC gene. For this study, the candidate gene approach was employed. The information about the selected gene of interest, *ARC*, was extracted from an online genetic database - (GRCh37.p13; https://www.ncbi.nlm.nih.gov/gene/23237). For the IMAGEN sample, there was only one SNP (rs10097505) located within the *ARC* gene locus. A total sample of 1315 was extracted from the IMAGEN cohort based on the availability of corresponding ESPAD measures.

In the human study, the significance of the associations with ESPAD variables of interest was corrected for multiple testing and established using permutations (n = 10000). The p-value (two-tailed) was computed by taking the absolute number of permutations that resulted in a higher correlation than the observed absolute value and divided by the total number of permutations. For the statistical tests corrected with permutations, the alpha level of 0.05 was applied, unless otherwise specified. Analyses of

associations between genotype and methylation were performed using the Statistical Package for the Social Science (IBM SPSS version 25), while analyses that included ESPAD variables of interest were computed in MATLAB (R2018a) using scripts generated for this study.

Statistical Analysis. All results are expressed as mean +/- SEM. The appropriate tests were chosen, taking into account whether data follow the normal distribution. Statistical analysis was performed in Graphpad Prism v.8, for Windows, GraphPad Software, La Jolla California USA. Details for each statistical test are marked in figure legends. Data were considered significantly different when $P < 0.05$.

Declarations

Acknowledgments, Funding and Disclosure. This work has been supported by the European Union's Horizon 2020 research and innovation programme under the Marie Sklodowska-Curie grant agreement no 665735 (Bio4Med) and by the funding from Polish Ministry of Science and Higher Education within 2016-2020 funds for the implementation of international projects (agreement no 3548/H2020/COFUND/2016/2) and National Science Centre (Poland) Harmonia and Opus grants (UMO-2016/22/M/NZ4/00674 and UMO-2015/19/B/NZ4/03163) to KR. This work was further supported by the German National Science Foundation (Deutsche Forschungsgemeinschaft [DFG]), grant MU 2789/8-2 and in part by the Federal Ministry of Education and Research (BMBF) under the e:Med Program (031L0190B and 01KC2004B) and by Japan Society for the Promotion of Science KAKENHI grants (17H06312 and 19H03328). This work received support from the following sources: the European Union-funded FP6 Integrated Project IMAGEN (Reinforcement-related behaviour in normal brain function and psychopathology) (LSHM-CT- 2007-037286), the Horizon 2020 funded ERC Advanced Grant 'STRATIFY' (Brain network based stratification of reinforcement-related disorders) (695313), Human Brain Project (HBP SGA 2, 785907, and HBP SGA 3, 945539), the Medical Research Council Grant 'c-VEDA' (Consortium on Vulnerability to Externalizing Disorders and Addictions) (MR/N000390/1), the National Institute of Health (NIH) (R01DA049238, A decentralized macro and micro gene-by-environment interaction analysis of substance use behavior and its brain biomarkers), the National Institute for Health Research (NIHR) Biomedical Research Centre at South London and Maudsley NHS Foundation Trust and King's College London, the Bundesministeriumfür Bildung und Forschung (BMBF grants 01GS08152; 01EV0711; Forschungsnetz AERIAL 01EE1406A, 01EE1406B; Forschungsnetz IMAC-Mind 01GL1745B), the Deutsche Forschungsgemeinschaft (DFG grants SM 80/7-2, SFB 940, TRR 265, NE 1383/14-1), the Medical Research Foundation and Medical Research Council (grants MR/R00465X/1 and MR/S020306/1), the National Institutes of Health (NIH) funded ENIGMA (grants 5U54EB020403-05 and 1R56AG058854-01), NSFC grant 82150710554 and environMENTAL grant. Further support was provided by grants from: - the ANR (ANR-12-SAMA-0004, AAPG2019 - GeBra), the Eranet Neuron (AF12-NEUR0008-01 - WM2NA; and ANR-18-NEUR00002-01-ADORe), the Fondation de France (00081242), the Fondation pour la Recherche Médicale (DPA20140629802), the Mission Interministérielle de Lutte-contre-les-Drogues-et-les-Conduites-Addictives (MILDECA), the Assistance-Publique-Hôpitaux-de-Paris and INSERM (interface grant), Paris Sud University IDEX 2012, the Fondation de l'Avenir (grant AP-RM-17-013), the Fédération pour la Recherche sur le Cerveau; the National Institutes of Health, Science Foundation Ireland (16/ERCD/3797),

U.S.A. (Axon, Testosterone and Mental Health during Adolescence; RO1 MH085772-01A1) and by NIH Consortium grant U54 EB020403, supported by a cross-NIH alliance that funds Big Data to Knowledge Centres of Excellence. ImagenPathways "Understanding the Interplay between Cultural, Biological and Subjective Factors in Drug Use Pathways" is a collaborative project supported by the European Research Area Network on Illicit Drugs (ERANID). This paper is based on independent research commissioned and funded in England by the National Institute for Health Research (NIHR) Policy Research Programme (project ref. PR-ST-0416-10001. The views expressed in this article are those of the authors and not necessarily those of the national funding agencies or ERANID.

Author contributions. KR initiated the studies, designed experiments, supervised and coordinated research; RP, AS, ES, AB, MNS, AC and KR performed and analyzed mouse studies; HO, HB and KK provided materials and supervised *in vitro* experiments; IMAGEN consortium, NT, JZ, GS and CPM analyzed human data. RP, CPM, GS and KR wrote the manuscript. All authors discussed the results and commented on the manuscript.

Conflict of interest. Tobias Banaschewski served in an advisory or consultancy role for eye level, Infectopharm, Lundbeck, Medice, Neurim Pharmaceuticals, Oberberg GmbH, Roche, and Takeda. He received conference support or speaker's fee by Janssen, Medice and Takeda. He received royalities from Hogrefe, Kohlhammer, CIP Medien, Oxford University Press; the present work is unrelated to these relationships. Dr Barker has received honoraria from General Electric Healthcare for teaching on scanner programming courses. Dr Poustka served in an advisory or consultancy role for Roche and Viforpharm and received a speaker's fee from Shire. She received royalties from Hogrefe, Kohlhammer and Schattauer. The present work is unrelated to the above grants and relationships. The other authors report no biomedical financial interests or potential conflicts of interest.

References

1. American Psychiatric Association, American Psychiatric Association, editors. Diagnostic and statistical manual of mental disorders: DSM-5. 5th ed. Washington, D.C: American Psychiatric Association; 2013.
2. Carvalho AF, Heilig M, Perez A, Probst C, Rehm J. Alcohol use disorders. The Lancet. 2019;394:781–792.
3. Sinha R. How Does Stress Lead to Risk of Alcohol Relapse? Alcohol Res. 2012;34:432–440.
4. Sinha R, Li CSR. Imaging stress- and cue-induced drug and alcohol craving: association with relapse and clinical implications. Drug Alcohol Rev. 2007;26:25–31.
5. Venniro M, Caprioli D, Shaham Y. Animal models of drug relapse and craving. Progress in Brain Research, vol. 224, Elsevier; 2016. p. 25–52.
6. Mantsch JR, Baker DA, Funk D, Lê AD, Shaham Y. Stress-Induced Reinstatement of Drug Seeking: 20 Years of Progress. Neuropsychopharmacology. 2016;41:335–356.

7. Crombag HS, Bossert JM, Koya E, Shaham Y. Context-induced relapse to drug seeking: a review. Philos Trans R Soc Lond B Biol Sci. 2008;363:3233–3243.
8. Ray LA, Roche DJO. Neurobiology of Craving: Current Findings and New Directions. Curr Addict Rep. 2018;5:102–109.
9. Ron D, Barak S. Molecular mechanisms underlying alcohol-drinking behaviours. Nat Rev Neurosci. 2016;17:576–591.
10. Stefaniuk M, Beroun A, Lebitko T, Markina O, Leski S, Meyza K, et al. Matrix Metalloproteinase-9 and Synaptic Plasticity in the Central Amygdala in Control of Alcohol-Seeking Behavior. Biological Psychiatry. 2017;81:907–917.
11. Warlow SM, Robinson MJF, Berridge KC. Optogenetic Central Amygdala Stimulation Intensifies and Narrows Motivation for Cocaine. J Neurosci. 2017;37:8330–8348.
12. Warlow SM, Naffziger EE, Berridge KC. The central amygdala recruits mesocorticolimbic circuitry for pursuit of reward or pain. Nat Commun. 2020;11:2716.
13. Douglass AM, Kucukdereli H, Ponserre M, Markovic M, Gründemann J, Strobel C, et al. Central amygdala circuits modulate food consumption through a positive-valence mechanism. Nat Neurosci. 2017;20:1384–1394.
14. Robinson MJF, Warlow SM, Berridge KC. Optogenetic excitation of central amygdala amplifies and narrows incentive motivation to pursue one reward above another. J Neurosci. 2014;34:16567–16580.
15. Radwanska K, Wrobel E, Korkosz A, Rogowski A, Kostowski W, Bienkowski P, et al. Alcohol relapse induced by discrete cues activates components of AP-1 transcription factor and ERK pathway in the rat basolateral and central amygdala. Neuropsychopharmacology. 2008;33:1835–1846.
16. Li X, Zeric T, Kambhampati S, Bossert JM, Shaham Y. The Central Amygdala Nucleus is Critical for Incubation of Methamphetamine Craving. Neuropsychopharmacology. 2015;40:1297–1306.
17. Kruzich PJ, See RE. Differential Contributions of the Basolateral and Central Amygdala in the Acquisition and Expression of Conditioned Relapse to Cocaine-Seeking Behavior. J Neurosci. 2001;21:RC155.
18. Lu L, Hope BT, Dempsey J, Liu SY, Bossert JM, Shaham Y. Central amygdala ERK signaling pathway is critical to incubation of cocaine craving. Nat Neurosci. 2005;8:212–219.
19. Knapska E, Radwanska K, Werka T, Kaczmarek L. Functional Internal Complexity of Amygdala: Focus on Gene Activity Mapping After Behavioral Training and Drugs of Abuse. Physiological Reviews. 2007;87:1113–1173.
20. Shepherd JD, Bear MF. New views of Arc, a master regulator of synaptic plasticity. Nat Neurosci. 2011;14:279–284.
21. Nikolaienko O, Patil S, Eriksen MS, Bramham CR. Arc protein: a flexible hub for synaptic plasticity and cognition. Seminars in Cell & Developmental Biology. 2018;77:33–42.

22. Plath N, Ohana O, Dammermann B, Errington ML, Schmitz D, Gross C, et al. Arc/Arg3.1 Is Essential for the Consolidation of Synaptic Plasticity and Memories. Neuron. 2006;52:437–444.
23. Shepherd JD, Rumbaugh G, Wu J, Chowdhury S, Plath N, Kuhl D, et al. Arc/Arg3.1 mediates homeostatic synaptic scaling of AMPA receptors. Neuron. 2006;52:475–484.
24. Chowdhury S, Shepherd JD, Okuno H, Lyford G, Petralia RS, Plath N, et al. Arc Interacts with the Endocytic Machinery to Regulate AMPA Receptor Trafficking. Neuron. 2006;52:445–459.
25. Nielsen LD, Pedersen CP, Erlendsson S, Teilum K. The Capsid Domain of Arc Changes Its Oligomerization Propensity through Direct Interaction with the NMDA Receptor. Structure. 2019;27:1071–1081.e5.
26. Alasmari F, Goodwani S, McCullumsmith RE, Sari Y. Role of glutamatergic system and mesocorticolimbic circuits in alcohol dependence. Prog Neurobiol. 2018;171:32–49.
27. Meyers JL, Salling MC, Almli LM, Ratanatharathorn A, Uddin M, Galea S, et al. Frequency of alcohol consumption in humans; the role of metabotropic glutamate receptors and downstream signaling pathways. Transl Psychiatry. 2015;5:e586.
28. Rao PSS, Bell RL, Engleman EA, Sari Y. Targeting glutamate uptake to treat alcohol use disorders. Frontiers in Neuroscience. 2015;9:144.
29. Eisenhardt M, Leixner S, Luján R, Spanagel R, Bilbao A. Glutamate Receptors within the Mesolimbic Dopamine System Mediate Alcohol Relapse Behavior. J Neurosci. 2015;35:15523–15538.
30. Radwanska K, Kaczmarek L. Characterization of an alcohol addiction-prone phenotype in mice: Characterization of an alcohol addiction-prone phenotype. Addiction Biology. 2012;17:601–612.
31. Cong L, Ran FA, Cox D, Lin S, Barretto R, Habib N, et al. Multiplex Genome Engineering Using CRISPR/Cas Systems. Science. 2013;339:819–823.
32. Schumann G, Loth E, Banaschewski T, Barbot A, Barker G, Büchel C, et al. The IMAGEN study: reinforcement-related behaviour in normal brain function and psychopathology. Mol Psychiatry. 2010;15:1128–1139.
33. Richardson NR, Roberts DC. Progressive ratio schedules in drug self-administration studies in rats: a method to evaluate reinforcing efficacy. J Neurosci Methods. 1996;66:1–11.
34. Epstein DH, Preston KL, Stewart J, Shaham Y. Toward a model of drug relapse: An assessment of the validity of the reinstatement procedure. Psychopharmacology (Berl). 2006;189:1–16.
35. Namba MD, Tomek SE, Olive MF, Beckmann JS, Gipson CD. The Winding Road to Relapse: Forging a New Understanding of Cue-Induced Reinstatement Models and Their Associated Neural Mechanisms. Front Behav Neurosci. 2018;12.
36. Deroche-Gamonet V. Evidence for Addiction-like Behavior in the Rat. Science. 2004;305:1014–1017.
37. Beroun A, Nalberczak-Skóra M, Harda Z, Piechota M, Ziółkowska M, Cały A, et al. Generation of silent synapses in dentate gyrus correlates with development of alcohol addiction. Neuropsychopharmacol. 2018;43:1989–1999.

38. Chen X, Nelson CD, Li X, Winters CA, Azzam R, Sousa AA, et al. PSD-95 Is Required to Sustain the Molecular Organization of the Postsynaptic Density. Journal of Neuroscience. 2011;31:6329–6338.
39. Sanjana NE, Shalem O, Zhang F. Improved vectors and genome-wide libraries for CRISPR screening. Genomics; 2014.
40. Nalberczak-Skóra M, Pattij T, Beroun A, Kogias G, Mielenz D, de Vries T, et al. Personality driven alcohol and drug abuse: New mechanisms revealed. Neuroscience & Biobehavioral Reviews. 2020;116:64–73.
41. Venniro M, Russell TI, Ramsey LA, Richie CT, Lesscher HMB, Giovanetti SM, et al. Abstinence-dependent dissociable central amygdala microcircuits control drug craving. Proc Natl Acad Sci U S A. 2020;117:8126–8134.
42. Kim J, Zhang X, Muralidhar S, LeBlanc SA, Tonegawa S. Basolateral to Central Amygdala Neural Circuits for Appetitive Behaviors. Neuron. 2017;93:1464–1479.e5.
43. Zakhari S. Alcohol metabolism and epigenetics changes. Alcohol Res. 2013;35:6–16.
44. Koob GF. Neurocircuitry of alcohol addiction. Handbook of Clinical Neurology, vol. 125, Elsevier; 2014. p. 33–54.
45. Abrahao KP, Salinas AG, Lovinger DM. Alcohol and the Brain: Neuronal Molecular Targets, Synapses, and Circuits. Neuron. 2017;96:1223–1238.
46. Morisot N, Ron D. Alcohol-dependent molecular adaptations of the NMDA receptor system. Genes Brain Behav. 2017;16:139–148.
47. Roberto M, Schweitzer P, Madamba SG, Stouffer DG, Parsons LH, Siggins GR. Acute and chronic ethanol alter glutamatergic transmission in rat central amygdala: an in vitro and in vivo analysis. J Neurosci. 2004;24:1594–1603.
48. Salling MC, Faccidomo SP, Li C, Psilos K, Galunas C, Spanos M, et al. Moderate Alcohol Drinking and the Amygdala Proteome: Identification and Validation of Calcium/Calmodulin Dependent Kinase II and AMPA Receptor Activity as Novel Molecular Mechanisms of the Positive Reinforcing Effects of Alcohol. Biol Psychiatry. 2016;79:430–442.
49. Wernicke C, Samochowiec J, Schmidt LG, Winterer G, Smolka M, Kucharska-Mazur J, et al. Polymorphisms in the N-methyl-D-aspartate receptor 1 and 2B subunits are associated with alcoholism-related traits. Biol Psychiatry. 2003;54:922–928.
50. Karpyak VM, Geske JR, Colby CL, Mrazek DA, Biernacka JM. Genetic variability in the NMDA-dependent AMPA trafficking cascade is associated with alcohol dependence. Addict Biol. 2012;17:798–806.
51. Bohnsack JP, Teppen T, Kyzar EJ, Dzitoyeva S, Pandey SC. The lncRNA BDNF-AS is an epigenetic regulator in the human amygdala in early onset alcohol use disorders. Transl Psychiatry. 2019;9:34.
52. Yakout DW, Shree N, Mabb AM. Effect of pharmacological manipulations on Arc function. Curr Res Pharmacol Drug Discov. 2021;2:100013.

53. Pandey SC, Zhang H, Ugale R, Prakash A, Xu T, Misra K. Effector Immediate-Early Gene Arc in the Amygdala Plays a Critical Role in Alcoholism. Journal of Neuroscience. 2008;28:2589–2600.
54. Managò F, Mereu M, Mastwal S, Mastrogiacomo R, Scheggia D, Emanuele M, et al. Genetic Disruption of Arc/Arg3.1 in Mice Causes Alterations in Dopamine and Neurobehavioral Phenotypes Related to Schizophrenia. Cell Reports. 2016;16:2116–2128.
55. Wall MJ, Collins DR, Chery SL, Allen ZD, Pastuzyn ED, George AJ, et al. The Temporal Dynamics of Arc Expression Regulate Cognitive Flexibility. Neuron. 2018;98:1124–1132.e7.
56. Penrod RD, Kumar J, Smith LN, McCalley D, Nentwig TB, Hughes BW, et al. Activity-regulated cytoskeleton-associated protein (Arc/Arg3.1) regulates anxiety- and novelty-related behaviors. Genes, Brain and Behavior. 2019;18:e12561.
57. Penrod RD, Thomsen M, Taniguchi M, Guo Y, Cowan CW, Smith LN. The activity-regulated cytoskeleton-associated protein, Arc/Arg3.1, influences mouse cocaine self-administration. Pharmacology Biochemistry and Behavior. 2020;188:172818.
58. Kyzar EJ, Zhang H, Pandey SC. Adolescent Alcohol Exposure Epigenetically Suppresses Amygdala Arc Enhancer RNA Expression to Confer Adult Anxiety Susceptibility. Biological Psychiatry. 2019;85:904–914.
59. Huentelman MJ, Muppana L, Corneveaux JJ, Dinu V, Pruzin JJ, Reiman R, et al. Association of SNPs in EGR3 and ARC with Schizophrenia Supports a Biological Pathway for Schizophrenia Risk. PLOS ONE. 2015;10:e0135076.
60. Alzheimer's Disease Neuroimaging Initiative, Bi R, Kong L-L, Xu M, Li G-D, Zhang D-F, et al. The Arc Gene Confers Genetic Susceptibility to Alzheimer's Disease in Han Chinese. Mol Neurobiol. 2018;55:1217–1226.
61. Penner MR, Roth TL, Chawla MK, Hoang LT, Roth ED, Lubin FD, et al. Age-related changes in Arc transcription and DNA methylation within the hippocampus. Neurobiology of Aging. 2011;32:2198–2210.
62. Wrase J, Makris N, Braus DF, Mann K, Smolka MN, Kennedy DN, et al. Amygdala Volume Associated With Alcohol Abuse Relapse and Craving. AJP. 2008;165:1179–1184.
63. Grace S, Rossetti MG, Allen N, Batalla A, Bellani M, Brambilla P, et al. Sex differences in the neuroanatomy of alcohol dependence: hippocampus and amygdala subregions in a sample of 966 people from the ENIGMA Addiction Working Group. Transl Psychiatry. 2021;11:156.
64. Hill SY, Bellis MDD, Keshavan MS, Lowers L, Shen S, Hall J, et al. Right amygdala volume in adolescent and young adult offspring from families at high risk for developing alcoholism. Biological Psychiatry. 2001;49:894–905.
65. Livak KJ, Schmittgen TD. Analysis of relative gene expression data using real-time quantitative PCR and the 2(-Delta Delta C(T)) Method. Methods. 2001;25:402–408.
66. Hirano Y, Ihara K, Masuda T, Yamamoto T, Iwata I, Takahashi A, et al. Shifting transcriptional machinery is required for long-term memory maintenance and modification in Drosophila mushroom bodies. Nat Commun. 2016;7:13471.

67. IMAGEN Consortium, Mielenz D, Reichel M, Jia T, Quinlan EB, Stöckl T, et al. EFhd2/Swiprosin-1 is a common genetic determinator for sensation-seeking/low anxiety and alcohol addiction. Mol Psychiatry. 2018;23:1303–1319.
68. Schilling S, DeStefano AL, Sachdev PS, Choi SH, Mather KA, DeCarli CD, et al. APOE genotype and MRI markers of cerebrovascular disease. Neurology. 2013;81:292–300.

Figures

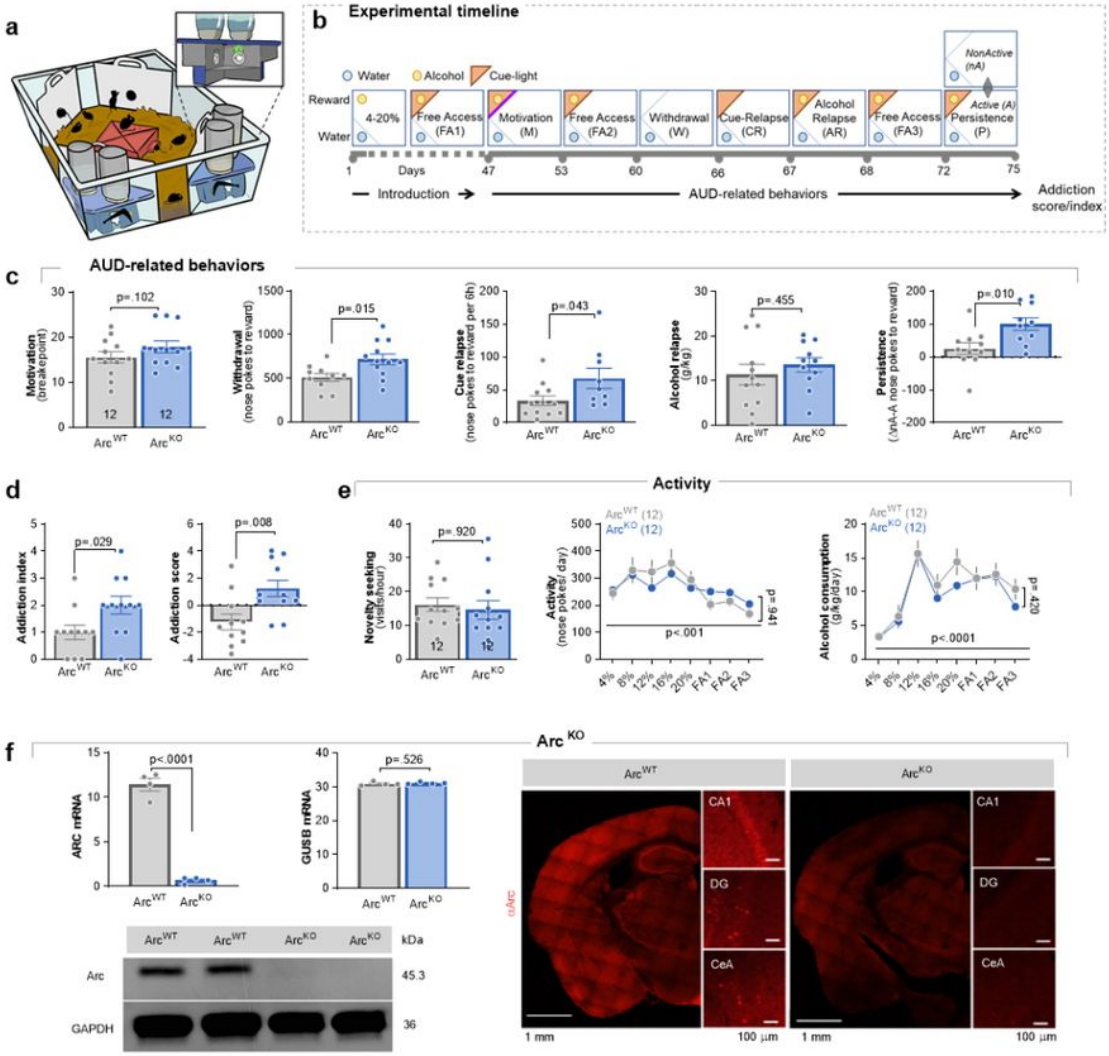

Figure 1

AUD-related behaviors in Arc^{KO} mice.

(a-b) IntelliCage setup (with a magnified cage corner) and the experimental timeline. Arc^{KO} (n=12) and Arc^{WT} (n=12) mice were trained to drink alcohol in the IntelliCage, AUD-related behaviors were tested, addiction score (sum of normalized scores from all AUD tests) and index (sum of positive results (top 35%) in all tests) were calculated. We analyzed motivation to drink alcohol (Motivation, M); alcohol craving during withdrawal (Withdrawal, W); reinstatement of alcohol seeking by alcohol-predicting cues (Cue relapse, CR); lack of control over alcohol consumption (Alcohol relapse, AR); and persistence of alcohol seeking (Persistence, P). (c) Summary of data showing individual scores in AUD-related behaviors: motivation to alcohol ($t_{(20)} = 2.013$, $p = 0.062$), persistence in alcohol seeking ($t_{(20)} = 2.844$, $p = 0.010$), alcohol seeking during withdrawal ($t_{(20)} = 2.293$, $p = 0.034$), alcohol seeking during cue relapse ($t_{(20)} = 2.160$, $p = 0.043$), and alcohol consumption during alcohol relapse ($t_{(20)} = 0.766$, $p = 0.455$). Each dot on the graphs represents one animal. Mean +/- SEM are shown. (d) Summary of data showing addiction score ($t_{(20)} = 2.954$, $p = 0.008$) and addiction index ($t_{(20)} = 2.345$, $p = 0.029$). (e) Mice general activity. Summary of data showing novelty seeking ($t_{(20)} = 0.101$, $p = 0.920$), activity in cage corners (repeated measure (RM) ANOVA, effect of genotype: $F_{(1, 20)} = 0.007$, $p = 0.932$) and alcohol consumption (RM ANOVA, effect of genotype: $F_{(1, 20)} = 0.714$, $p = 0.408$). (f) The analysis of Arc mRNA and protein expression in Arc KO and Arc WT mice. (top) Arc and Gusb mRNA levels in Arc^{KO} mice and Arc^{WT} (Arc: $t_{(6)} = 14.84$, $p < 0.001$; GUSB: $t_{(6)} = 0.672$, $p = 0.526$). (left, bottom) Arc KO mice expressed no Arc protein in the brain. GAPDH was used as a loading control for WB. (right) Representative micro-photography of Arc immunostaining in Arc^{KO} and Arc^{WT} mice after 90-minute novel context exposure. DG, dentate gyrus; CA1, CA1 area of the hippocampus; CeA, central nucleus of the amygdala

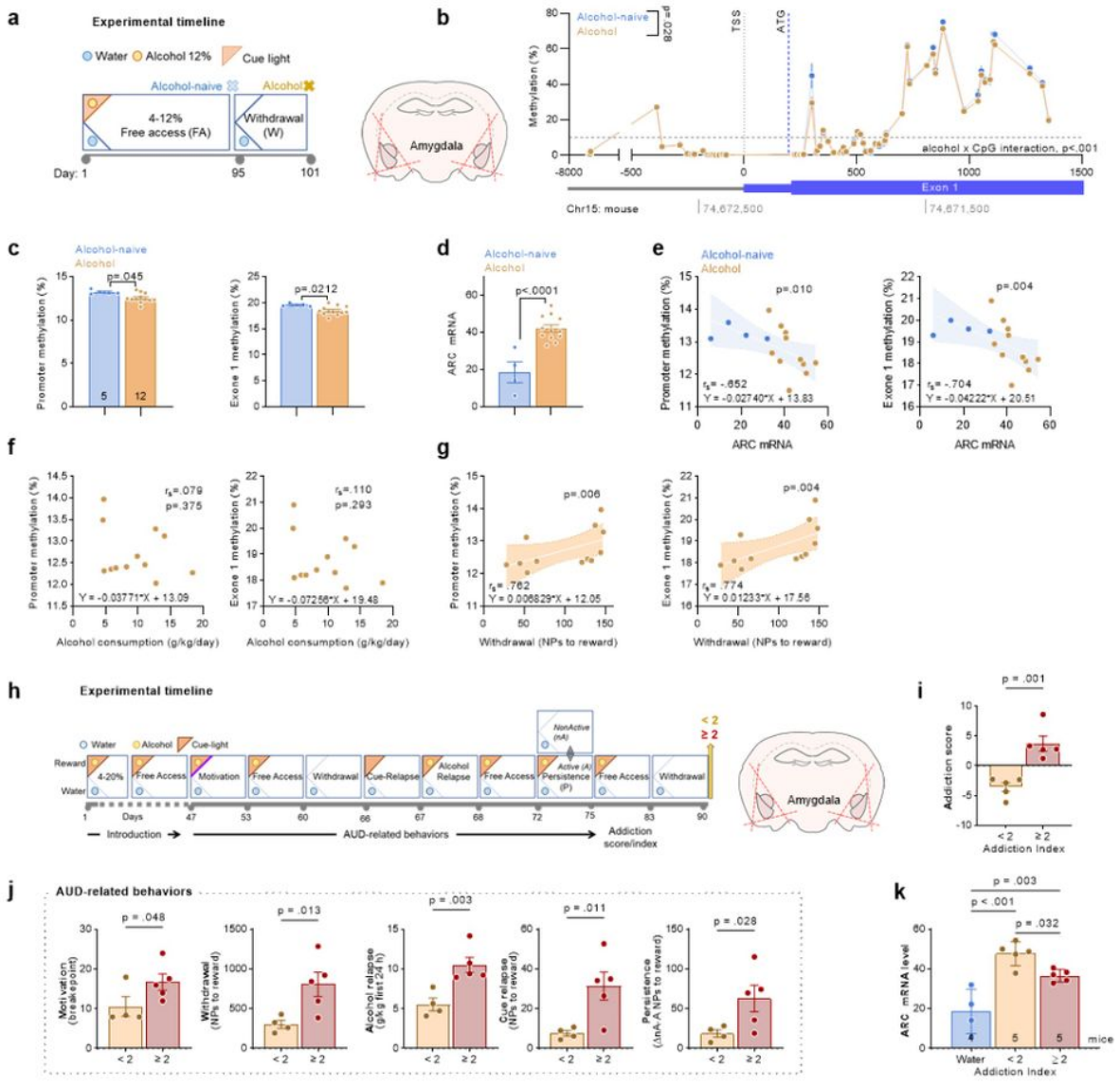

Figure 2

Alcohol consumption decreases Arc gene methylation and increases Arc mRNA expression in the mouse amygdala. (a) Experimental design. Mice had free access to 10% alcohol in the IntelliCages for 95 days and were sacrificed after 6-day alcohol withdrawal. The amygdala tissue was dissected and used to analyze DNA methylation Arc mRNA levels. (b) The analysis of methylation frequency in 54 CpG within Arc promoter and exon 1 (for CpGs with methylation > 10%; repeated measure (RM) ANOVA, effect of alcohol: $F_{(1, 16)} = 6.84$, $p = 0.018$; effect of CpG: $F_{(3.469, 55.50)} = 183.2$, $p < 0.0001$; alcohol x CpG interaction: $F_{(20, 320)} = 1.810$, $p = 0.0189$). (c-e) Summary of data showing (c) the average methylation of

Arc promoter (Mann-Whitney U = 11, p = 0.045) and exon 1 (Mann-Whitney U = 8.50, p = 0.021) CpGs, (d) Arc mRNA levels ($t_{(14)}$ = 5.152, p < 0.001) and (e) correlation of Arc mRNA levels and Arc gene methylation (promoter and exon 1) in the amygdala of alcohol-naïve and alcohol trained mice (Spearman correlation; r_s, Spearman r). Regression lines and 95% confidence intervals are shown. Each dot represents one mouse. (f-g) Summary of data showing correlation of Arc gene methylation (promoter and exon 1) in the amygdala of alcohol trained mice with (f) alcohol consumption and (g) alcohol seeking during withdrawal (Spearman correlation; rs , Spearman r). Regression lines and 95% confidence intervals are shown. Each dot represents one mouse. (h-r) Transcriptomic analysis of AUD-prone and resistant animals. (h) Experimental timeline. C57BL/6J mice were trained in the IntelliCage. (i) Addiction score was calculated based on five AUD-related behaviors. AUD-prone (≥ 2) and resistant (< 2) animals were identified (t(8) = 4.98, p = 0.001). (j) AUD-related behaviors: motivation for alcohol (Unpaired t-test, t(7)= 1.93, p = 0.048), alcohol seeking during withdrawal (t(7)= 2.82, p = 0.013), and cue-induced relapse (t(7)= 2.96, p = 0.011), alcohol relapse (t(7)= 3.81, p = 0.003) and persistence tests (t(7)= 2.28, p = 0.028). (k) Summary of data showing Arc mRNA expression in the amygdala of AUD-prone and -resistant animals (one-way ANOVA with post-hoc LSD tests, F(2, 11) = 18.6, p < 0.001).

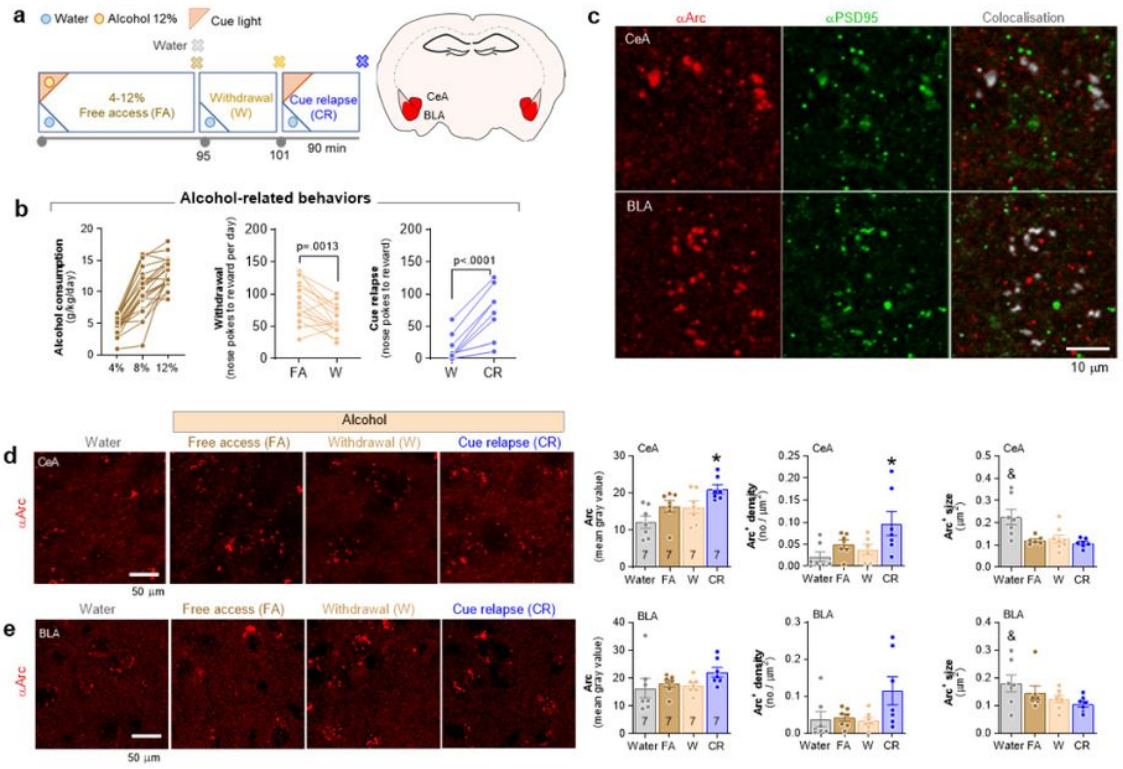

Figure 3

Arc protein is upregulated in the CeA during cue relapse. (a) Experimental timeline and schematic drawing of the central (CeA) and basolateral nuclei of the amygdala (BLA). Mice were trained to drink alcohol (Alcohol) or water (Water) in the IntelliCages and were sacrificed at three time-points: free access period (Water/Alcohol, n = 7/7), withdrawal (n = 7) and cue-induced relapse (n = 7). Brain sections were immunostained to detect Arc and PSD-95 proteins. (b) Summary of data showing: (left) alcohol consumption, and (middle) alcohol seeking during withdrawal (W), as compared to day before the test (FA) (paired t-test, $t_{(14)} = 3.99$, $p = 0.001$); and (right) during cue relapse (CR) as compared to day before the test (W) (paired t-test, $t_{(7)} = 5.823$, $p < 0.001$). (c) Representative microphotographs showing fluorescent immunostaining for Arc, PSD-95 and their colocalization, in the CeA and BLA of an alcohol-naïve mouse. (d-e) Representative microphotographs and summary of data showing Arc expression in CeA and BLA (pictures/mice, Water: 37/7, Alcohol, FA: 34/7, W: 39/7, CR: 36/7) (CeA: one way ANOVA, MGV: $F(3, 24) = 5.76$, $p = 0004$; density: $F(3, 23) = 3.79$, $p = 0.024$; size: $F(3, 24) = 6.85$, $p = 00017$; BLA: one way ANOVA, MGV: $F(3, 24) = 1.421$, $p = 0.261$; density: $F(3, 24) = 2.892$, $p = 0.056$; size: $F(3, 25) = 2.355$, $p = 0.096$). *$p < 0.05$ for CR vs other groups, &$p < 0.05$ for Water vs other groups, by Tukey's post hoc tests. Data is presented as means +/- SEM.

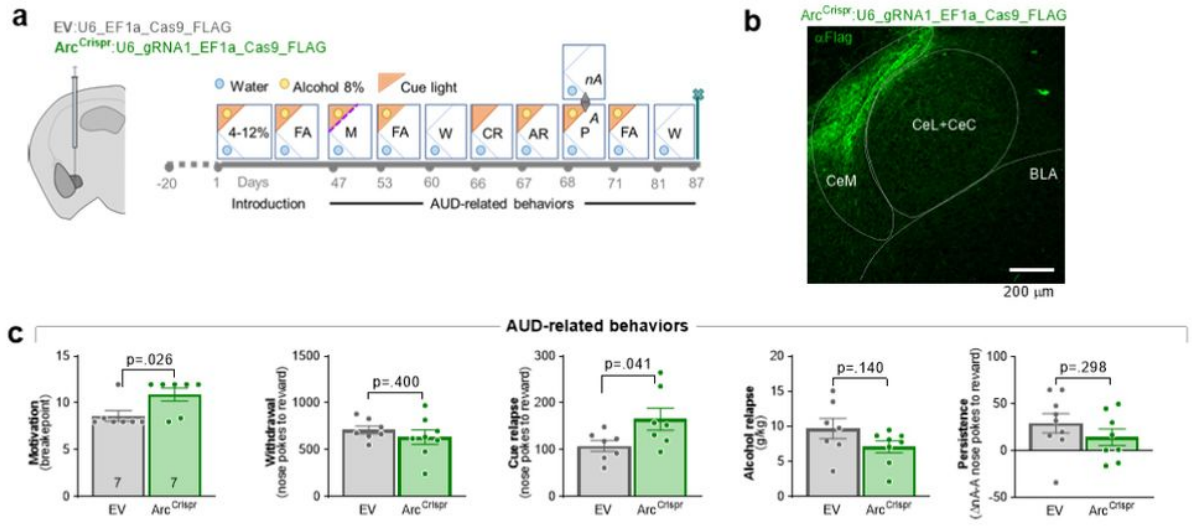

Figure 4

Downregulation of Arc in CeM increases motivation and alcohol seeking during relapse induced by alcohol-predicting cues.

(a) Experimental timeline. Mice had bilateral stereotactic injections of Arc^{Crispr} (n=7) or EV (n=7) (200 nl, titer: 10^7 -10^8 GC/ µl) into CeM, and three weeks later they were trained to drink alcohol in the IntelliCages and AUD-related behaviors were assessed. (b) A representative micro-photography of Flag immunostaining in CeM after Arc^{Crispr} injection The post-training analysis of the brain sections confirmed that Arc^{Crispr} and EV were expressed in CeM. The post-training analysis of the brain sections. (c) Summary of data showing AUD-related behaviors: motivation test ($t_{(13)}$ = 2.077, p = 0.026), withdrawal ($t_{(13)}$ = 0.870, p = 0.400), cue relapse ($t_{(13)}$ = 2.18, p = 0.041), alcohol relapse ($t_{(13)}$ = 0.230, p = 0.140) and a persistence test ($t_{(13)}$ = 0.083, p = 0.298). Data is presented as means and SEM. Each dot on the graphs represents one animal.

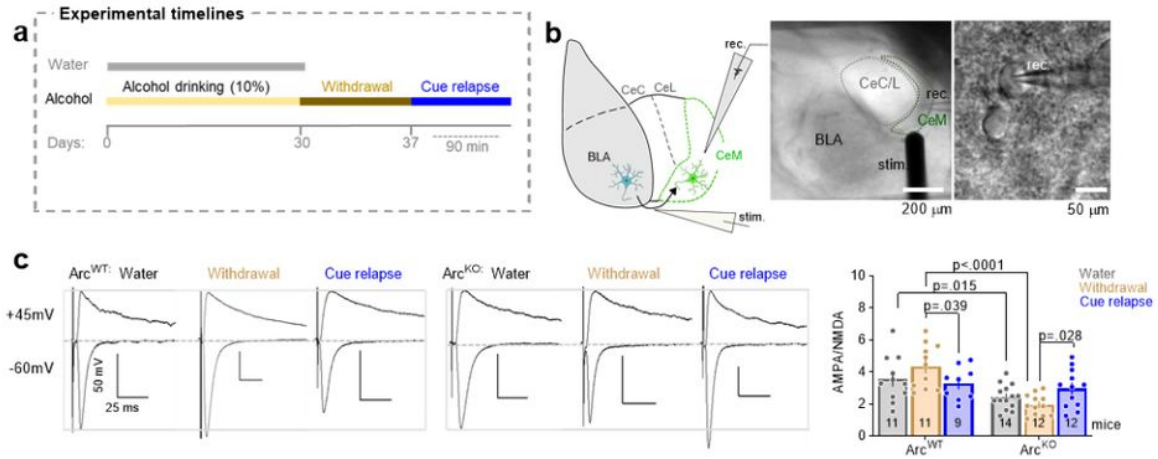

Figure 5

Arc regulates synaptic strength of BLA→CeM pathway during cue relapse.

(a) Experimental timeline. Arc^{KO} and Arc^{WT} mice were trained for 30 days to drink alcohol in home cages. Mice were sacrificed after 7-day withdrawal from alcohol, after 90 minutes of cue relapse or alcohol-naïve mice were used. (b) Experimental design and representative microphotographs of the amygdala and a patched cell in CeM. Whole-cell patch-clamp recordings were performed on the CeM cells with the stimulation electrode placed at the axons from BLA. (c) The analysis of AMPA/NMDA EPSCs in the BLA→CeM pathway. (left) Representative EPSCs traces and (right) summary of data showing

AMPA/NMDA EPSCs in Arc^{WT} and Arc^{KO} mice (two-way ANOVA, training x genotype effect: F(2, 63) = 4.94, p = 0.010; effect of genotype: F(1, 63) = 22.85, p < 0.0001; effect of training: F(2, 63) = 0.137, p = 0.872; with LSD post hoc tests). Data is presented as means +/- SEM.

a

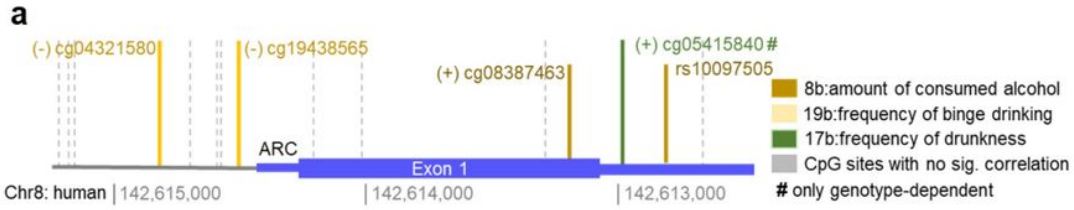

b

		Right Amygdala	Left Amygdala	Right Hippocampus	Left Hippocampus
cg08387463	Correlation	*r* = - 0.022	***r* = - 0.087***	*r* = - 0.046	*r* = - 0.015
	Sig. (2-tailed)	*p* = 0.612	***p* = 0.044**	*p* = 0.293	*p* = 0.724
cg04321580	Correlation	*r* = 0.041	*r* = 0.017	*r* = 0.031	*r* = 0.052
	Sig. (2-tailed)	*p* = 0.344	*p* = 0.705	*p* = 0.476	*p* = 0.236
cg19438565	Correlation	*r* = 0.028	*r* = - 0.016	*r* = 0.009	*r* = 0.027
	Sig. (2-tailed)	*p* = 0.519	*p* = 0.713	*p* = 0.843	*p* = 0.544

Figure 6

Alcohol consumption affects ARC gene methylation.

(a) Alcohol-related behavioral variables (ESPAD: alcohol consumption: 8b, frequency of drunkenness: 17b, binge drinking: 19b) correlate with a single nucleotide polymorphism (SNP, rs10097505, variant: G>A) and methylation of four (cg05415840, cg08387463, cg04321580 and cg19438565), out of fifteen, CpG sites within the ARC gene. N = 1315. (-) Negative and (+) positive correlations. A purple rectangle shows the exon; the thick rectangle represents the coding part, thin - non-coding part. (b) Analysis of the correlation of ARC gene methylation sites and volume of amygdala and hippocampus. r, Pearson correlation coefficient.

Supplementary Files

This is a list of supplementary files associated with this preprint. Click to download.

- PaganosupplementaryMolPSych1.pdf